ACCEPTED MANUSCRIPT - Online First - Available Online: June 06, 2022

SCFs in multi-planar tubular TT-joints of offshore jacket structures subjected to out-of plane bending (OPB) loads

Hamid Ahmadi*[,1,2], Hossein Imani[1]

[1]*Faculty of Civil Engineering, University of Tabriz, Tabriz 5166616471, Iran*
[2]*Center of Excellence in Hydroinformatics, Faculty of Civil Engineering, University of Tabriz, Tabriz, Iran*

*Corresponding Author

E-mail Addresses: h-ahmadi@tabrizu.ac.ir (H. Ahmadi); husenimani@gmail.com (H. Imani)

Abstract

Investigating the effect of loaded out-of-plane braces on the values of the stress concentration factor (SCF) in offshore tubular joints has been the objective of numerous research works. However, due to the diversity of joint types and loading conditions, a number of quite important cases still exist that have not been studied thoroughly. Among them are two-planar TT-joints subjected to out-of-plane bending (OPB) moment loading. In the present research, data extracted from the stress analysis of 243 finite element (FE) models, verified against available experimental data, was used to study the effects of geometrical parameters on the chord-side SCFs in two-planar tubular TT-joints subjected to two types of OPB moment loading. Parametric FE study was followed by a set of nonlinear regression analyses to develop four new SCF parametric formulae for OPB-loaded two-planar TT-joints. Reliability of proposed equations was checked against UK DoE criteria.

Keywords: Out-of-plane bending (OPB); Stress concentration factor (SCF); Two-planar tubular TT-joint; Fatigue; Offshore jacket structure.

1. Introduction

Offshore jacket-type platforms are widely used for the production of oil and gas from hydrocarbon reservoirs below the seabed (Fig. 1a). Primary structural part of an offshore jacket-type platform is fabricated from tubular members by welding one end of the branch member, i.e. brace, to the undisturbed surface of the main member, i.e. chord, resulting in what is known as a tubular joint (Fig. 1b). The static and fatigue strength of tubular joints are the governing factors in the design of jacket structures.

Since the significant stress concentrations at the vicinity of the welds are considerably detrimental to the fatigue performance of the joints, it is important to accurately determine the magnitude of stress concentration and to reduce it to a reasonable level. In the design practice, a parameter called the stress concentration factor (SCF) is used to evaluate the magnitude of the stress concentration. The SCF, defined as the ratio of the local surface stress at the brace-to-chord intersection to the nominal stress in the brace, exhibits considerable scatter depending on the joint geometry, loading type, weld size and type, and the considered position for the SCF calculation around the weld profile.

Under any specific loading condition, the SCF value along the weld toe of a tubular joint is mainly determined by the joint geometry. To study the behavior of tubular joints and to easily relate this behavior to the geometrical characteristics of the joint, a set of dimensionless geometrical parameters has been defined. Fig. 1c depicts a two-planar tubular TT-joint with the geometrical parameters τ, γ, β, α, and α_B where D and d are the diameters of the chord and brace, respectively; L and l are the lengths of those members, respectively; and T and t are the chord and brace thickness, respectively. Critical positions along the weld toe of the brace-to-chord intersection for the calculation of SCFs in a tubular joint, i.e. saddle and crown, have been shown in Fig. 1c.

Over the past fifty years, significant effort has been devoted to the study of SCFs in various uniplanar tubular joints (i.e. joints where the axes of the chord and brace members lay on the same plane). As a result, many parametric design formulas in terms of the joint's geometrical parameters have been proposed providing SCF values at certain positions adjacent to the weld for several loading conditions. Multi-planar joints (i.e. joints where the axes of the chord and all brace members do not lay on the same plane) are an intrinsic feature of offshore tubular structures. The multi-planarity effect might play an important role in the stress distribution along the brace-to-chord intersection. Thus for multi-planar connections, the parametric formulae of simple uniplanar tubular joints may not be applicable for the SCF prediction; since such formulae may lead to highly over- or under-predicting results. Nevertheless, for multi-planar joints which cover the majority of practical applications, much fewer investigations have been reported due to the complexity and high cost involved.

Results of a numerical investigation on the SCFs in two-planar tubular TT-joints, also called multi-planar DT-joints, are discussed in the present paper. In this research program, a set of parametric finite element (FE) stress analyses was carried out on 81 tubular TT-joint models subjected to two types of out-of-plane bending (OPB) moment loading (Fig. 2). Analysis results were used to present general remarks on the effects of geometrical parameters including τ (brace-to-chord thickness ratio), γ (chord wall slenderness ratio), β (brace-to-chord diameter ratio), and α (chord length-to-radius ratio) on the SCFs at the saddle positions. Crown positions were not studied. The reason is that under the OPB moment loading, the stress at these positions is nearly zero and hence the determination of SCF values at the crown positions does not have a practical value. Based on the results of TT-joint FE models, verified against experimental data, an SCF database was prepared. Then, a new set of SCF parametric equations was established, based on nonlinear regression analyses, for the fatigue analysis and design of two-planar tubular TT-joints subjected to OPB moment loading. The reliability of proposed equations was evaluated according to the acceptance criteria recommended by the UK DoE [1].

Appropriate place for the insertion of Figs. 1 & 2

2. Literature review

2.1. Calculation of SCFs in uniplanar tubular joints

For investigating the SCFs in unstiffened uniplanar tubular joints, the reader is referred to Kuang et al. [2], Efthymiou [3], Hellier et al. [4], UK HSE OTH 354 [5], and Karamanos et al. [6] for the SCF calculation at the saddle and crown positions of simple uniplanar T-, Y-, X-, K-, and KT-joints; and Gho and Gao [7], Gao [8], Gao et al. [9], and Yang et al. [10] for the SCF determination in overlapped uniplanar joints, among others.

For the study of SCF distribution along the weld toe in unstiffened uniplanar tubular joints, the reader is referred for example to Morgan and Lee [11, 12] for K-joints; Chang and Dover [13, 14] for T-, Y-, X-, and DT-joints; Shao [15, 16] and Shao et al. [17] for T- and K-joints; Lotfollahi-Yaghin and Ahmadi [18], Ahmadi et al. [19], and Lotfollahi-Yaghin and Ahmadi [20] for KT- and DKT-joints; and Liu et al. [21] for T-joints.

For the SCF calculation at saddle and crown positions of stiffened tubular joints, the reader is referred for example to Nwosu et al. [22] for ring-stiffened T-joints; Hoon et al. [23] for doubler-plate reinforced T-joints; Myers et al. [24] for rack-plate reinforced joints; Ahmadi and Lotfollahi-Yaghin [25] and Ahmadi and Zavvar [26] for ring-stiffened KT-joints subjected to in-plane bending (IPB) moment and OPB moment loadings; Xu et al. [27] for concrete-filled joints; Nassiraei and Rezadoost [28–33] for FRP-strengthened T/Y- and X-joints subjected to axial and bending loads; and Ahmadi and Khavaninzadeh [34] for doubler-plate reinforced X-joints.

Ahmadi et al. [35, 36] investigated the SCF distribution along the weld toe of central and outer braces in tubular KT-joints reinforced with internal ring stiffeners and proposed a set of parametric equations to calculate the SCFs along the brace-to-chord intersection in internally ring-stiffened KT-joints subjected to axial loading.

2.2. Calculation of SCFs in multi-planar tubular joints

For the SCF studies in unstiffened multi-planar joints, the reader is referred to Karamanos et al. [37] and Chiew et al. [38] for the SCF calculation in XX-joints; Wingerde et al. [39] for the SCF determination in KK-joints; Karamanos et al. [40] for the study of SCFs in DT-joints; Chiew et al. [41] for the study of SCFs in XT-joints; Ahmadi et al. [42, 43], Ahmadi and Lotfollahi-Yaghin [44], and Ahmadi and Zavvar [45] for the investigation of SCFs in multi-planar KT-joints under axial loads; and Ahmadi and Kouhi [46] for the SCF determination in unreinforced XT-joints subjected to out-of-plane bending (OPB) moment loadings, among others.

Woghiren and Brennan [47] developed a set of parametric equations to predict the SCFs at critical positions along the brace-to-chord intersection in two-planar tubular KK-joints reinforced with rack plates. Ahmadi et al. [48] studied the stress concentration in internally ring-stiffened two-planar tubular KK-joints. Ahmadi and Imani [49] investigated the SCFs in offshore two-planar tubular TT-joints reinforced with internal ring stiffeners.

2.3. Other SCF-related investigations in various tubular joints

For other SCF-related studies such as probabilistic and reliability studies, the reader is referred for example to Ahmadi et al. [50], Gaspar et al. [51], Ahmadi and Lotfollahi-Yaghin [52, 53], Ahmadi et al. [54, 55], Ahmadi [56], and Ahmadi and Mousavi Nejad Benam [57].

2.4. Remarks

From Sect. 2.1–2.3, it can be clearly concluded that, over the past five decades, significant effort has been devoted to the study of SCFs in various uniplanar joints. However, the study of SCFs in multi-planar joints is rather limited. Despite the use of two-planar tubular TT-joints in the design of offshore jacket-type structures, the SCFs in OPB-loaded TT-joints have not been investigated and no design equation is currently available to determine the weld-toe SCFs at the saddle positions in tubular TT-joints subjected to OPB moment loading.

3. FE modeling and SCF extraction

3.1. Weld profile

One of the most critical factors affecting the accuracy of SCF results is the accurate modeling of the weld profile. Therefore, the weld sizes must be carefully included in the FE modeling. A number of research works has been carried out on the study of the weld effect. For example, the reader is referred to Lee and Wilmshurst

[58], Cao et al. [59], and Lee [60], among others. It was found that the fatigue strength of the joint can be underestimated by 20% compared to the experimental data without considering the weld [61].

In the present research, the welding size along the brace-to-chord intersection satisfies the AWS D 1.1 [62] specifications. However, it should be noted that attempts to produce an improved as-welded profile often result in over-welding. Consequently, the actual weld size, typical of yard practice, is usually different from the nominal weld size recommended by AWS D 1.1 [62]. For the correction of SCFs to consider the actual position of the weld toe, the reader is advised to follow the recommendations of Section C 5.3.2(a) of API RP 2A [63].

It should be noted that, considering the effect of possible weld defects, the hot-spot stress (HSS) method has been quite efficient and popular for fatigue design purposes. According to this method, the nominal stress at the joint members is multiplied by an appropriate SCF to provide the HSS at a certain location. HSSs are calculated at various positions around the weld and the maximum HSS range (S) is determined. Then, the fatigue life of the joint is estimated through an appropriate S–N fatigue curve, N being the number of load cycles. The HSS range concept places different structural geometries on a common basis, enabling them to be treated using a single S–N curve. The basis of this concept is to capture a stress (or strain) in the proximity of the weld toes, which characterizes the fatigue life of the joint, but excludes the very local microscopic effects like the sharp notch, undercut and crack-like defects at the weld toe. These local weld notch effects are included in the S–N curve.

The dihedral angle (ψ) which is an important parameter in determining the weld thickness is defined as the angle between the chord and brace surface along the intersection curve. The dihedral angle at the two typically important positions along the weld toe, i.e. saddle and crown, equals to π–$\cos^{-1}(\beta)$ and $\pi/2$, respectively. Details of weld profile modeling according to AWS D 1.1 [62] have been presented by Ahmadi et al. [43].

3.2. Boundary conditions

The chord end fixity conditions of tubular joints in offshore structures may range from almost fixed to almost pinned with generally being closer to almost fixed [3]. In practice, the value of the parameter α in over 60% of tubular joints is in excess of 20 and is bigger than 40 in 35% of the joints [64]. Changing the end restraint from fixed to pinned results in a maximum increase of 15% in the SCF at the crown position for joints with $\alpha = 6$, and this increase reduces to only 8% for $\alpha = 8$ [12]. In the view of the fact that the effect of chord end restraints is only significant for joints with $\alpha < 8$ and high β and γ values, which do not commonly occur in practice, both chord ends were assumed to be fixed, with the corresponding nodes restrained.

Due to the symmetry in geometry and loading of the joint, only half of the entire tubular TT-joint is required to be modeled in order to reduce the computational time (Fig. 3). Appropriate symmetric boundary conditions were defined for the nodes located on the symmetry planes.

Appropriate place for the insertion of Fig. 3

3.3. Mesh generation

In the present study, ANSYS element SOLID95 was used to model the chord, braces, and weld profiles. This element type has compatible displacements and is well-suited to model curved boundaries. It is defined by 20 nodes having three degrees of freedom per node and may have any spatial orientation. Using this type of 3-D brick elements, the weld profile can be modeled as a sharp notch. This method will produce more accurate and detailed stress distribution near the intersection in comparison with a shell analysis.

To guarantee the mesh quality, a sub-zone mesh generation scheme was used during the FE modeling. The entire structure was divided to several zones according to computational requirements. The mesh of each zone

was generated separately and then the mesh of the entire joint was produced by merging the meshes of all the sub-zones. This scheme can feasibly control the mesh quantity and quality and avoid badly distorted elements. The mesh generated by this procedure for a tubular TT-joint is shown in Fig. 4a.

As mentioned earlier, in order to determine the SCF, the stress at the weld toe should be divided by the nominal stress of the loaded brace. The stresses perpendicular to the weld toe at the extrapolation points are required to be calculated in order to determine the stress at the weld toe position. To extract and extrapolate the stresses perpendicular to the weld toe, as shown in Figs. 4b and 5b, the region between the weld toe and the second extrapolation point was meshed finely in such a way that each extrapolation point was placed between two nodes located in its immediate vicinity. These nodes are located on the element-generated paths which are perpendicular to the weld toe.

In order to verify the convergence of FE results, convergence test with different mesh densities was conducted before generating the 81 FE models for the parametric study.

Appropriate place for the insertion of Fig. 4

3.4. Analysis and the SCF determination

Static analysis of the linearly elastic type is suitable to determine the SCFs in tubular joints [65]. The Young's modulus and Poisson's ratio were taken to be 207 GPa and 0.3, respectively.

The weld-toe SCF at the saddle position is defined as:

$$\text{SCF} = \sigma_{\perp W} / \sigma_n \tag{1}$$

In Eq. (1), σ_n is the nominal stress of the OPB-loaded brace which is calculated as follows:

$$\sigma_n = \frac{32 d M_o}{\pi\left[d^4 - \left(d - 2t\right)^4\right]} \tag{2}$$

where M_o is the out-of-plane bending moment; and d and t are brace diameter and thickness, respectively.

To calculate the SCF, the stress at the weld toe position should be extracted from the stress field outside the region influenced by the local weld toe geometry. The location from which the stresses have to be extrapolated, *extrapolation region*, depends on the dimensions of the joint and on the position along the intersection. According to the linear extrapolation method recommended by IIW-XV-E [66], the first extrapolation point must be at a distance of $0.4T$ from the weld toe, and the second point should lie at $1.0T$ further from the first point (Fig. 5a). In Eq. (1), $\sigma_{\perp W}$ is the extrapolated stress at the weld toe position which is perpendicular to the weld toe and is calculated by the following equation:

$$\sigma_{\perp W} = 1.4\sigma_{\perp E1} - 0.4\sigma_{\perp E2} \tag{3}$$

where $\sigma_{\perp E1}$ and $\sigma_{\perp E2}$ are the stresses at the first and second extrapolation points along the direction perpendicular to the weld toe, respectively.

The stress at an extrapolation point is obtained as follows:

$$\sigma_{\perp E} = \frac{\sigma_{\perp N1} - \sigma_{\perp N2}}{\delta_1 - \delta_2}\left(\Delta - \delta_2\right) + \sigma_{\perp N2} \tag{4}$$

where $\sigma_{\perp Ni}$ (i = 1 and 2) is the nodal stress at the immediate vicinity of the extrapolation point along the direction perpendicular to the weld toe at the saddle position (Eq. (5)); δ_i (i = 1 and 2) is the distance between

the weld toe and the considered node inside the extrapolation region (Eq. (6)); and Δ equals to $0.4T$ and $1.4T$ for the first and second extrapolation points, respectively (Fig. 5b).

$$\sigma_{\perp N} = \sigma_y m_1^2 + \sigma_z n_1^2 + 2\tau_{yz} m_1 n_1 \tag{5}$$

$$\delta = \sqrt{\left(x_w - x_n\right)^2 + \left(y_w - y_n\right)^2 + \left(z_w - z_n\right)^2} \tag{6}$$

In Eq. (6), (x_n , y_n , z_n) and (x_w , y_w , z_w) are the global coordinates of the considered node inside the extrapolation region and its corresponding node at the weld toe position, respectively. In Eq. (5), components of the stress tensor can be extracted from ANSYS analysis results; and m_1 and n_1 are transformation components calculated as follows:

$$m_1 = \left(y_w - y_n\right)/\delta \; ; \; n_1 = \left(z_w - z_n\right)/\delta \tag{7}$$

To facilitate the SCF calculation, above formulation was implemented in a *macro* developed by the ANSYS Parametric Design Language (APDL). The input data required to be provided by the user of the macro are the node number at the weld toe, the chord thickness, and the numbers of the nodes inside the extrapolation region. These nodes can be introduced using the Graphic user interface (GUI).

Appropriate place for the insertion of Fig. 5

3.5. FE model verification

As far the authors are aware, there is no experimental/numerical data available in the literature on the SCFs in OPB-loaded two-planar tubular TT-joints that are studied in the present research. However, a set of related experimental data is available that can be used to verify the present FE models.

To validate the present FE models, experimental data on the SCFs of uniplanar T-joints published in HSE OTH 354 [5] was used. In order to do so, an FE model was generated for a T-joint having the same geometrical characteristics as the T704/1 specimen (Table 1) and the model was analyzed subjected to the brace OPB moment loading (Fig. 6). The method of geometrical modeling (introducing the chord, brace, and weld profile), the mesh generation procedure (including the selection of element type and size), load application, analysis method, and the method of SCF extraction are identical for the T-joint validating model and the TT-joint models used for the parametric study. Hence, the verification of SCF values derived from validating FE model with the experimental data from HSE OTH 354 [5] lends some support to the validity of SCF values derived from the FE models of present paper. Result of verification process presented in Table 2 shows that there is a good agreement between the results of present FE model and HSE OTH 354 [5] experimental data. Hence, generated FE models can be considered to be accurate enough to provide valid results.

Appropriate place for the insertion of Tables 1 & 2 and Fig. 6

4. Geometrical effects on the SCFs

To study the SCFs in two-planar tubular TT-joints subjected to two types of OPB moment loading (Fig. 2), 81 models were generated and analyzed using the FE software, ANSYS (Ver. 19). The objective was to investigate the effects of dimensionless geometrical parameters on the chord-side SCFs at the saddle positions.

Values assigned to parameters β, γ, τ, and α have been presented in Table 3. These values cover the practical ranges of the dimensionless parameters typically found in tubular joints of offshore jacket structures. The brace length has no effect on SCFs when the parameter α_B is greater than a critical value [14]. In the present

study, in order to avoid the effect of short brace length, a realistic value of $\alpha_B = 8$ was assigned to all joints. The 81 generated models span the following ranges of the geometric parameters:

$$\begin{aligned} &0.3 \le \beta \le 0.5 \\ &12 \le \gamma \le 24 \\ &0.4 \le \tau \le 1.0 \\ &8 \le \alpha \le 24 \end{aligned} \tag{10}$$

Appropriate place for the insertion of Table 3

Two charts are given in Fig. 7, as an example, depicting the change of chord-side SCFs at the inner saddle (IS) and outer saddle (OS) positions due to the change in the value of the τ and the interaction of this parameter with the γ under the 1st OPB moment loading condition. The parameter τ is the ratio of brace thickness to chord thickness and the γ is the ratio of radius to thickness of the chord. Hence, the increase of the τ in models having constant value of the γ results in the increase of the brace thickness. Under each loading condition, a large number comparative charts were used to study the effect of the τ on the SCFs at the IS and OS positions and only two of them are presented here for the sake of brevity. Results showed that under both studied loading conditions, the increase of the τ leads to the increase of SCFs at all the saddle positions. This result is not dependent on the values of other geometrical parameters.

Fig. 8 demonstrates the change of the SCFs at the IS and OS positions due to the change in the value of the β and the interaction of this parameter with the α under the 1st OPB moment loading condition. The parameter β is the ratio of brace diameter to chord diameter. Hence, the increase of the β in models having constant value of chord diameter results in the increase of brace diameter. Through investigating the effect of the β on the SCFs, it can be concluded that the change of the β generally leads to the increase of the SCFs at the both saddle positions. This conclusion is not dependent on either the values of other geometrical parameters or the type of axial loading.

Two charts are presented in Fig. 9 depicting the change of SCFs at the IS and OS positions due to the change in the value of the γ and the interaction of this parameter with the β under the 1st OPB moment loading condition. The parameter γ is the ratio of radius to thickness of the chord. Hence, the increase of the γ in models having constant value of the chord diameter means the decrease of chord thickness. It was observed that under both studied loading conditions, the increase of the γ results in the increase of SCFs at the saddle positions.

Fig. 10 shows the change of the SCF values at the IS and OS positions due to the change in the value of the α and the interaction of this parameter with the γ under the 1st OPB moment loading condition. The parameter α is the ratio of the length to the radius of the chord. Hence, the increase of the α in models having constant value of the chord diameter means the increase of the chord length. Results showed that the increase of the α does not have a considerable effect on the SCF values at the inner and outer saddle positions. This results are not dependent on either the values of other geometrical parameters or the type of OPB moment loading.

Appropriate place for the insertion of Figs. 7–10

5. Effects of loading type, position, and multi-planarity on the SCFs

A sample set of six two-planar TT-joints was selected (Table 4) to depict the differences among the SCFs at the IS and OS positions under the two types of OPB moment loading condition shown in Fig. 2. Results given in Table 5 show that the SCFs at the inner saddle position under the 1st OPB moment loading condition are the biggest values observed. By comparing the SCFs at the considered saddle positions, it can be concluded that:

1st OPB moment loading condition: $SCF_{IS} > SCF_{OS}$ (11)

2nd OPB moment loading condition: $SCF_{OS} > SCF_{IS}$ (12)

The uniplanar and multi-planar SCF values are compared in Fig. 11 indicating that there can be a quite big difference between the SCF values in uniplanar and two-planar T-joints. For example, under the 1st OPB moment loading condition, the SCF value at the inner saddle position of TT42 model (β = 0.4, γ = 18, τ = 1.0, α = 16) is 2.6 times the SCF at the saddle position of the corresponding uniplanar T-joint. Hence, it can be concluded that for OPB-loaded two-planar TT-joints, the parametric formulas of simple uniplanar T-joints are not applicable for the SCF prediction, since such formulas may lead to highly under-predicting results. Consequently, developing a set of specific parametric equations for the SCF calculation in two-planar TT-joints has practical value.

Appropriate place for the insertion of Fig. 11 and Tables 4 & 5

6. Development of parametric formulae for the SCF determination

Four individual parametric equations are proposed in the present paper, to calculate the SCFs at the saddle positions on the weld toe of two-planar tubular TT-joints subjected to OPB moment loading.

To develop these parametric SCF design formulae, results of multiple nonlinear regression analyses performed by SPSS were used. Values of dependent variable (i.e. SCF) and independent variables (i.e. β, γ, τ, and α) constitute the input data imported in the form of a matrix. Each row of this matrix involves the information about the SCF value at a saddle position on the weld toe of a two-planar tubular TT-joint having specific geometrical properties.

After defining the dependent and independent variables, a model expression must be built with defined parameters. Parameters of the model expression are unknown coefficients and exponents. The researcher must specify a starting value for each parameter, preferably as close as possible to the expected final solution. Poor starting values can result in failure to converge or in convergence on a solution that is local (rather than global) or is physically impossible. Various model expressions must be built to derive a parametric equation having a high coefficient of determination (R^2).

After performing a large number of nonlinear analyses, following parametric equations are proposed for the calculation of chord-side SCFs at the saddle positions in two-planar tubular TT-joints subjected to the two considered OPB moment loading conditions (Fig. 2):

- ***1st OPB moment loading condition:***

Inner saddle position:

$$SCF_{1st\text{-}IS} = 0.793\,\beta^{1.083}\gamma^{1.329}\tau^{0.896}\alpha^{-0.011} \quad ; \quad R^2 = 0.998 \tag{13}$$

Outer saddle position:

$$SCF_{1st\text{-}OS} = 0.381\,\beta^{0.596}\gamma^{1.289}\tau^{0.848}\alpha^{0.020} \quad ; \quad R^2 = 0.995 \tag{14}$$

- ***2nd OPB moment loading condition:***

Inner saddle position:

$$SCF_{2nd\text{-}IS} = 0.427\,\beta^{0.658}\gamma^{1.173}\tau^{0.859}\alpha^{0.119} \quad ; \quad R^2 = 0.987 \tag{15}$$

Outer saddle position:

$$SCF_{2nd\text{-}OS} = 0.895\,\beta^{1.141}\gamma^{1.225}\tau^{0.910}\alpha^{0.073} \quad ; \quad R^2 = 0.996 \tag{16}$$

Values obtained for R^2 are quite high indicating the accuracy of the fit. The validity ranges of dimensionless geometrical parameters for the developed equations have been given in Eq. (10).

The SCF values predicted by proposed equations are compared with the SCFs extracted from FE analyses in Fig. 12. It can be seen that there is a good agreement between the results of proposed equations and numerically computed values.

The UK Department of Energy (DoE) [1] recommends the following assessment criteria regarding the applicability of the commonly used SCF parametric equations (P/R stands for the ratio of the *predicted* SCF from a given equation to the *recorded* SCF from test or analysis):

- For a given dataset, if % SCFs under-predicting $\leq$ 25%, i.e. [%P/R < 1.0] $\leq$ 25%, and if % SCFs considerably under-predicting $\leq$ 5%, i.e. [%P/R < 0.8] $\leq$ 5%, then accept the equation. If, in addition, the percentage SCFs considerably over-predicting $\leq$ 50%, i.e. [%P/R > 1.5] $\geq$50%, then the equation is regarded as generally conservative.
- If the acceptance criteria is nearly met i.e. 25% < [%P/R < 1.0] $\leq$ 30%, and/or 5% < [%P/R < 0.8] $\leq$ 7.5%, then the equation is regarded as borderline and engineering judgment must be used to determine acceptance or rejection.
- Otherwise reject the equation as it is too optimistic.

In view of the fact that for a mean fit equation, there is always a large percentage of under-prediction, the requirement for joint under-prediction, i.e. P/R < 1.0, can be completely removed in the assessment of parametric equations [67]. Assessment results according to the UK DoE [1] criteria are presented in Table 6 showing that all equations satisfy the criteria recommended by the UK Department of Energy.

Appropriate place for the insertion of Fig. 12 and Table 6

7. Conclusions

Results of stress analyses performed on 81 FE models verified against experimental data were used to investigate the effects of geometrical parameters on the chord-side SCFs at the saddle positions in two-planar tubular TT-joints, also called multi-planar DT-joints, under two types of OPB moment loading. A set of SCF parametric equations was also developed for the fatigue design. Main conclusions are summarized as follows.

The increase of the parameters τ, β, and γ leads to the increase of the SCFs at the saddle positions. The change of the α does not have a considerable effect on the SCF values at the inner and outer saddle positions.

The SCFs at the inner saddle position under the 1st OPB moment loading condition are the biggest values observed. There can be a quite big difference between the SCF values in uniplanar T- and two-planar TT-joints. Hence, for OPB-loaded two-planar TT-joints, the parametric formulae of simple uniplanar T-joints are not applicable for the SCF prediction, since such formulas may lead to highly under-predicting results. Consequently, developing a set of specific parametric equations for the SCF calculation in two-planar TT-joints has practical value. High coefficients of determination and the satisfaction of acceptance criteria recommended by the UK DoE guarantee the accuracy of four parametric equations proposed in the present paper. Hence, the developed equations can reliably be used for the fatigue analysis and design of two-planar tubular TT-joints subjected to OPB moment loading.

References

[1] UK Department of Energy (DoE). Background notes to the fatigue guidance of offshore tubular joints. UK DoE, London, UK; 1983.

[2] Kuang JG, Potvin AB, Leick RD. Stress concentration in tubular joints. Proceedings of the Offshore Technology Conference, Paper OTC 2205, Houston (TX), US; 1975.

[3] Efthymiou M. Development of SCF formulae and generalized influence functions for use in fatigue analysis. OTJ 88, Surrey, UK; 1988.

[4] Hellier AK, Connolly M, Dover WD. Stress concentration factors for tubular Y and T-joints. Int J Fatigue 1990;12:13–23.

[5] UK Health and Safety Executive (HSE). OTH 354: Stress concentration factors for simple tubular joints − assessment of existing and development of new parametric formulae. UK HSE, London, UK; 1997.

[6] Karamanos SA, Romeijn A, Wardenier J. Stress concentrations in tubular gap K-joints: mechanics and fatigue design. Eng Struct 2000;22:4–14.

[7] Gho WM, Gao F. Parametric equations for stress concentration factors in completely overlapped tubular K(N)-joints. J Constr Steel Res 2004;60:1761–82.

[8] Gao F. Stress and strain concentrations of completely overlapped tubular joints under lap brace OPB load. Thin-Walled Struct 2006;44:861–71.

[9] Gao F, Shao YB, Gho WM. Stress and strain concentration factors of completely overlapped tubular joints under lap brace IPB load. J Constr Steel Res 2007;63: 305–16.

[10] Yang J, Chen Y, Hu K. Stress concentration factors of negative large eccentricity tubular N-joints under axial compressive loading in vertical brace. Thin-Walled Struct 2015;96:359−71.

[11] Morgan MR, Lee MMK. Parametric equations for distributions of stress concentration factors in tubular K-joints under out-of-plane moment loading. Int J Fatigue 1998;20:449–61.

[12] Morgan MR, Lee MMK. Prediction of stress concentrations and degrees of bending in axially loaded tubular K-joints. J Constr Steel Res 1998;45(1):67–97.

[13] Chang E, Dover WD. Prediction of stress distributions along the intersection of tubular Y and T-joints. Int J Fatigue 1999;21: 361–81.

[14] Chang E, Dover WD. Parametric equations to predict stress distributions along the intersection of tubular X and DT-joints. Int J Fatigue 1999;21:619–35.

[15] Shao YB. Proposed equations of stress concentration factor (SCF) for gap tubular K-joints subjected to bending load. Int J Space Struct 2004;19:137–47.

[16] Shao YB. Geometrical effect on the stress distribution along weld toe for tubular T- and K-joints under axial loading. J Constr Steel Res 2007;63:1351–60.

[17] Shao YB, Du ZF, Lie ST. Prediction of hot spot stress distribution for tubular K-joints under basic loadings. J Constr Steel Res 2009;65:2011–26.

[18] Lotfollahi-Yaghin MA, Ahmadi H. Effect of geometrical parameters on SCF distribution along the weld toe of tubular KT-joints under balanced axial loads. Int J Fatigue 2010;32:703–19.

[19] Ahmadi H, Lotfollahi-Yaghin MA, Aminfar MH. Geometrical effect on SCF distribution in uni-planar tubular DKT-joints under axial loads. J Constr Steel Res 2011;67:1282–91.

[20] Lotfollahi-Yaghin MA, Ahmadi H. Geometric stress distribution along the weld toe of the outer brace in two-planar tubular DKT-joints: parametric study and deriving the SCF design equations. Mar Struct 2011;24:239–60.

[21] Liu G, Zhao X, Huang Y. Prediction of stress distribution along the intersection of tubular T-joints by a novel structural stress approach. Int J Fatigue 2015; 80:216−30.

[22] Nwosu DI, Swamidas ASJ, Munaswamy K. Numerical stress analysis of internal ring-stiffened tubular T-joints. J Offshore Mech Arct 1995;117: 113–25.

[23] Hoon KH, Wong LK, Soh AK. Experimental investigation of a doubler-plate reinforced tubular T-joint subjected to combined loadings. J Constr Steel Res 2001;57:1015–39.

[24] Myers PT, Brennan FP, Dover WD. The effect of rack/rib plate on the stress concentration factors in jack-up chords. Mar Struct 2001;14: 485–505.

[25] Ahmadi H, Lotfollahi-Yaghin MA. Stress concentration due to in-plane bending (IPB) loads in ring-stiffened tubular KT-joints of offshore structures: Parametric study and design formulation. Appl Ocean Res 2015;51:54–66.

[26] Ahmadi H, Zavvar E. Stress concentration factors induced by out-of-plane bending loads in ring-stiffened tubular KT-joints of jacket structures. Thin-Walled Struct 2015;91:82–95.

[27] Xu F, Chen J, Jin W. Experimental investigation of SCF distribution for thin-walled concrete-filled CHS joints under axial tension loading. Thin-Walled Struct 2015;93:149−57.

[28] Nassiraei H, Rezadoost P. SCFs in tubular X-connections retrofitted with FRP under in-plane bending load. Compos Struct 2021;274:114314.

[29] Nassiraei H, Rezadoost P. SCFs in tubular X-joints retrofitted with FRP under out-of-plane bending moment. Mar Struct 2021;79:103010.

[30] Nassiraei H, Rezadoost P. Stress concentration factors in tubular X-connections retrofitted with FRP under compressive load. Ocean Eng 2021;229:108562.

[31] Nassiraei H, Rezadoost P. Parametric study and formula for SCFs of FRP-strengthened CHS T/Y-joints under out-of-plane bending load. Ocean Eng 2021; 221:108313.

[32] Nassiraei H, Rezadoost P. Stress concentration factors in tubular T/Y-connections reinforced with FRP under in-plane bending load. Mar Struct 2021;76:102871.

[33] Nassiraei H, Rezadoost P. Stress concentration factors in tubular T/Y-joints strengthened with FRP subjected to compressive load in offshore structures. Int J Fatigue 2020;140:105719.

[34] Ahmadi H, Khavaninzadeh MH. SCF distribution along the weld toe in tubular X-joints reinforced with doubler plates subjected to axial loading: Study of geometrical effects and design formulation. J Civ Environ Eng 2022; In Press.

[35] Ahmadi H, Lotfollahi-Yaghin MA, Shao YB, Aminfar MH. Parametric study and formulation of outer-brace geometric stress concentration factors in internally ring-stiffened tubular KT-joints of offshore structures. Appl Ocean Res 2012;38:74−91.

[36] Ahmadi H, Lotfollahi-Yaghin MA, Shao YB. Chord-side SCF distribution of central brace in internally ring-stiffened tubular KT-joints: A geometrically parametric study. Thin-Walled Struct 2013;70:93−105.

[37] Karamanos SA, Romeijn A, Wardenier J. Stress concentrations in multi-planar welded CHS XX-connections. J Constr Steel Res 1999;50:259–82.

[38] Chiew SP, Soh CK, Wu NW. General SCF design equations for steel multiplanar tubular XX-joints. Int J Fatigue 2000;22:283–93.

[39] Wingerde AM, Packer JA, Wardenier J. Simplified SCF formulae and graphs for CHS and RHS K- and KK-connections. J Constr Steel Res 2001;57:221–52.

[40] Karamanos SA, Romeijn A, Wardenier J. SCF equations in multi-planar welded tubular DT-joints including bending effects. Mar Struct 2002;15:157–73.

[41] Chiew SP, Soh CK, Wu NW. Experimental and numerical stress analyses of tubular XT-joint. J Struct Eng 1999;125:1239–48.

[42] Ahmadi H, Lotfollahi-Yaghin MA, Aminfar MH. Distribution of weld toe stress concentration factors on the central brace in two-planar CHS DKT-connections of steel offshore structures. Thin-Walled Struct 2011;49:1225–36.

[43] Ahmadi H, Lotfollahi-Yaghin MA, Aminfar MH. The development of fatigue design formulas for the outer brace SCFs in offshore three-planar tubular KT-joints. Thin-Walled Struct 2012;58:67–78.

[44] Ahmadi H, Lotfollahi-Yaghin MA. Geometrically parametric study of central brace SCFs in offshore three-planar tubular KT-joints. J Constr Steel Res 2012;71:149–61.

[45] Ahmadi H, Zavvar E. The effect of multi-planarity on the SCFs in offshore tubular KT-joints subjected to in-plane and out-of-plane bending loads. Thin-Walled Struct 2016;106:148–65.

[46] Ahmadi H, Kouhi A. Stress concentration factors of multi-planar tubular XT-joints subjected to out-of-plane bending moments. Appl Ocean Res 2020;96:102058.

[47] Woghiren CO, Brennan FP. Weld toe stress concentrations in multi planar stiffened tubular KK Joints. Int J Fatigue 2009;31:164–72.

[48] Ahmadi H, Alinezhad R, Alizadeh Atalo A. Stress concentration analysis of internally ring stiffened two-planar tubular KK-joints. Ships Offshore Struct 2021; In Press.

[49] Ahmadi H, Imani H. SCFs in offshore two-planar tubular TT-joints reinforced with internal ring stiffeners. Ocean Syst Eng 2022;12(1):1–22.

[50] Ahmadi H, Lotfollahi-Yaghin MA, Aminfar MH. Effect of stress concentration factors on the structural integrity assessment of multi-planar offshore tubular DKT-joints based on the fracture mechanics fatigue reliability approach. Ocean Eng 2011;38:1883−93.

[51] Gaspar B, Garbatov Y, Guedes Soares C. Effect of weld shape imperfections on the structural hot-spot stress distribution. Ships Offshore Struct 2011;6(1−2):145–59.

[52] Ahmadi H, Lotfollahi-Yaghin MA. A probability distribution model for stress concentration factors in multi-planar tubular DKT-joints of steel offshore structures. Appl Ocean Res 2012;34:21−32.

[53] Ahmadi H, Lotfollahi-Yaghin MA. Effect of SCFs on S–N based fatigue reliability of multi-planar tubular DKT-joints of offshore jacket-type structures. Ships Offshore Struct 2013;8:55−72.

[54] Ahmadi H. Mohammadi AH, Yeganeh A. Probability density functions of SCFs in internally ring-stiffened tubular KT-joints of offshore structures subjected to axial load. Thin-Walled Struct 2015;94:485–99.

[55] Ahmadi H. Mohammadi AH, Yeganeh A, Zavvar E. Probabilistic analysis of stress concentration factors in tubular KT-joints reinforced with internal ring stiffeners under in-plane bending loads. Thin-Walled Struct 2016;99:58–75.

[56] Ahmadi H. A probability distribution model for SCFs in internally ring-stiffened tubular KT-joints of offshore structures subjected to out-of-plane bending loads. Ocean Eng 2016;116:184–99.

[57] Ahmadi H, Mousavi Nejad Benam MA. Probabilistic analysis of SCFs in unstiffened gap tubular KT-joints of jacket structures under the OPB moment loads. Adv Struct Eng 2017;20:595–615.

[58] Lee MK, Wilmshurst SR. Numerical modeling of CHS joints with multiplanar double-K configuration. J Constr Steel Res 1995;32:281–301.

[59] Cao JJ, Yang GJ, Packer JA. FE mesh generation for circular tubular joints with or without cracks. Proceedings of the 7th International Offshore and Polar Engineering Conference, Honolulu (HI), US; 1997.

[60] Lee MMK. Strength, stress and fracture analyses of offshore tubular joints using finite elements. J Constr Steel Res 1999; 51:265–86.

[61] Shao YB. Fatigue behaviour of uni-planar CHS gap K-joints under axial and in-plane bending loads. PhD Thesis, School of Civil & Environmental Engineering, Nanyang Technological University, Singapore; 2004.

[62] American Welding Society (AWS). Structural welding code: AWS D 1.1. Miami (FL), US; 2002.

[63] American Petroleum Institute (API). Recommended practice for planning, designing and constructing fixed offshore platforms: Working stress design: RP 2A-WSD. 21st Edition, Errata and Supplement 3, Washington DC, US; 2007.

[64] Smedley P, Fisher P. Stress concentration factors for simple tubular joints. Proceedings of the International Offshore and Polar Engineering Conference (ISOPE), Edinburgh; 1991. p. 475–83.

[65] N'Diaye A, Hariri S, Pluvinage G, Azari Z. Stress concentration factor analysis for notched welded tubular T-joints. Int J Fatigue 2007;29:1554–70.

[66] IIW-XV-E. Recommended fatigue design procedure for welded hollow section joints, IIW Docs, XV-1035-99/XIII-1804-99. International Institute of Welding, France; 1999.

[67] Bomel Consulting Engineers. Assessment of SCF equations using Shell/KSEPL finite element data. C5970R02.01 REV C; 1994.

Table 1. Properties of uniplanar tubular T-joint used for the verification of present FE model

Joint ID [5]	Material	Loading type	D (mm)	τ	β	γ	α
T704/1	Steel	OPB moment	168	0.51	0.53	13.4	17.1

Table 2. Results of the FE model verification based on HSE OTH 354 [5] experimental data

Position	SCF		Difference
	Present FE model	Experimental data [5]	
Saddle	5.9	5.4	8.47%

Table 3. Values assigned to each dimensionless parameter

Parameter	Definition	Value(s)
β	d/D	0.3, 0.4, 0.5
γ	$D/2T$	12, 18, 24
τ	t/T	0.4, 0.7, 1.0
α	$2L/D$	8, 16, 24
α_B	$2l/d$	8

Table 4. Geometrical properties of TT-joints used for the comparison of SCFs under different loading conditions

Joint ID	D (mm)	τ	β	γ	α	α_B
TT1	500	0.4	0.3	12	24	8
TT15	500	1.0	0.4	18	24	8
TT26	500	0.7	0.5	24	24	8
TT47	500	0.7	0.3	24	16	8
TT69	500	0.7	0.4	18	8	8
TT81	500	1.0	0.5	24	8	8

Table 5. Comparing the SCFs under the two types of OPB moment loading condition

Joint ID	1st OPB moment loading condition		2nd OPB moment loading condition	
	IS	OS	IS	OS
TT1	2.70	2.25	2.23	2.67
TT15	13.62	10.01	9.97	13.56
TT26	17.86	11.58	11.94	18.24
TT47	10.29	8.67	8.49	10.13
TT69	13.70	9.90	9.09	12.68
TT81	25.09	15.28	12.91	21.79

Table 6. Results of formulae assessment according to the UK DoE [1] acceptance criteria

Proposed formulae	Conditions		Decision
	$\%P/R < 0.8$	$\%P/R > 1.5$	
Eq. (13)	0% < 5% OK.	0% < 50% OK.	Accept
Eq. (14)	0% < 5% OK.	0% < 50% OK.	Accept
Eq. (15)	0% < 5% OK.	0% < 50% OK.	Accept
Eq. (16)	0% < 5 % OK.	0% < 50% OK.	Accept

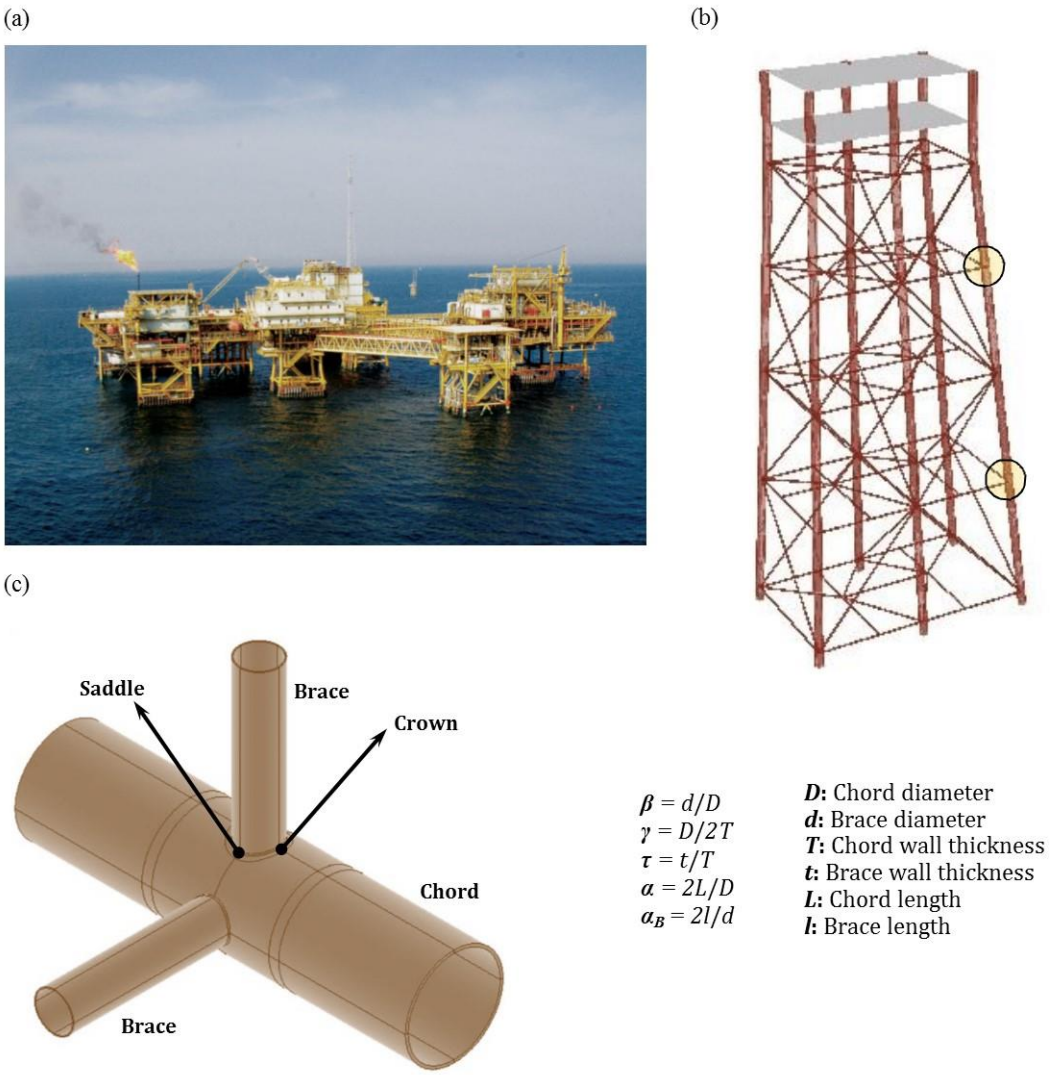

Fig. 1. (a) Jacket-type offshore platforms during service, (b) Two-planar tubular DT-joints in a jacket structure, (c) Geometrical notation for a multi-planar tubular TT-joint

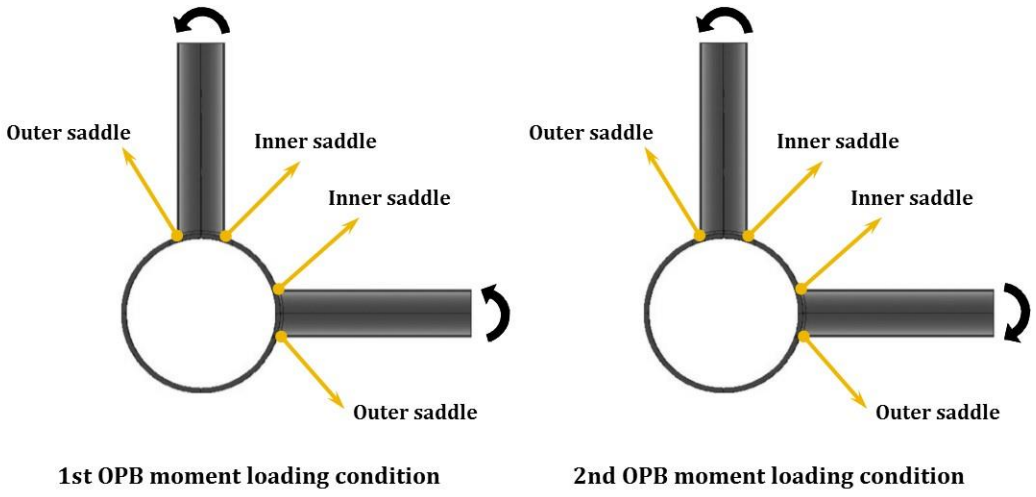

Fig. 2. Studied OPB moment loading conditions

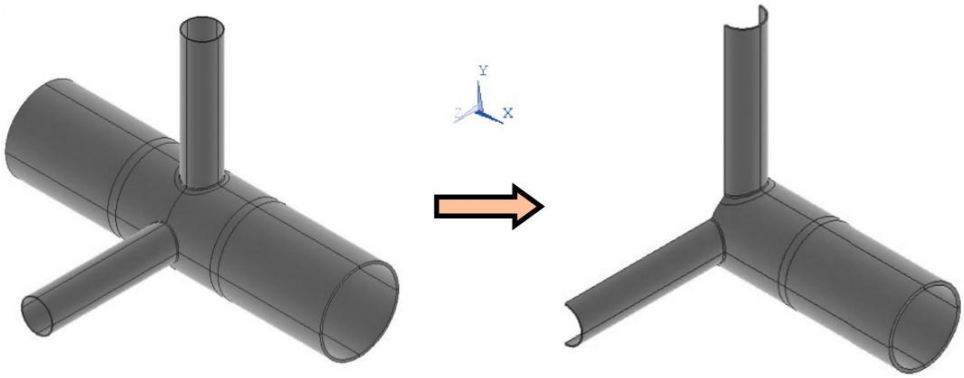

Fig. 3. One quarter of the entire two-planar TT-joint that is required to be modeled under studied OPB moment loading conditions

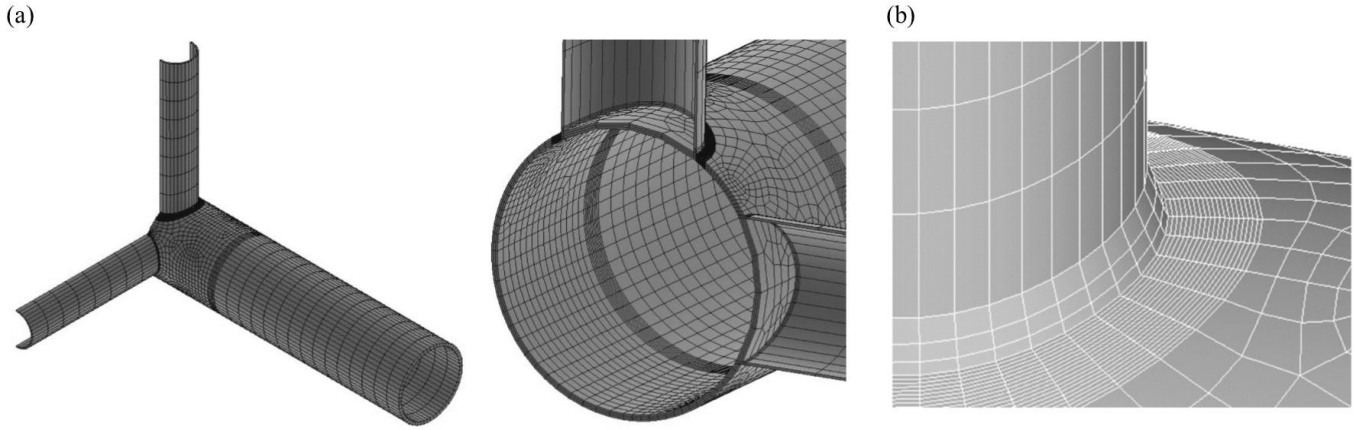

Fig. 4. Generated mesh by the sub-zone scheme: (a) Half of the joint under the OPB moment loading condition, (b) Regions adjacent to the brace-to-chord intersection

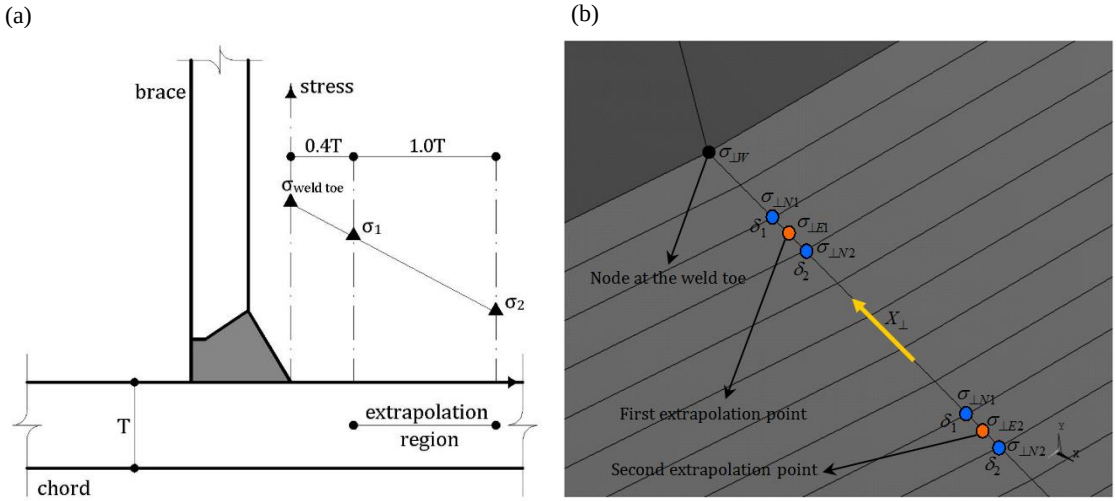

Fig. 5. (a) Extrapolation method according to IIW XV-E [66], (b) Required interpolations and extrapolations to extract the HSS value at the weld toe

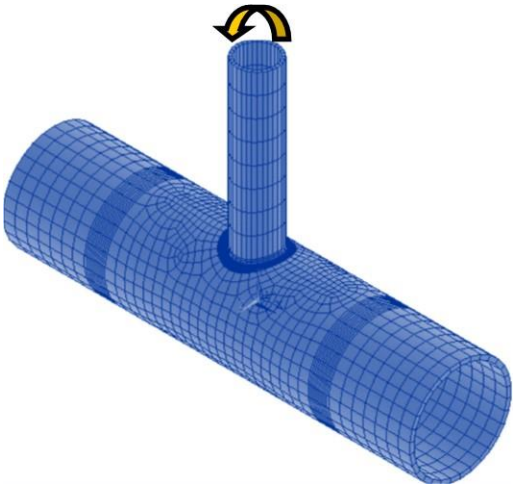

Fig. 6. Validating FE model generated for the comparison of the results with HSE OTH 354 [5] experimental measurements

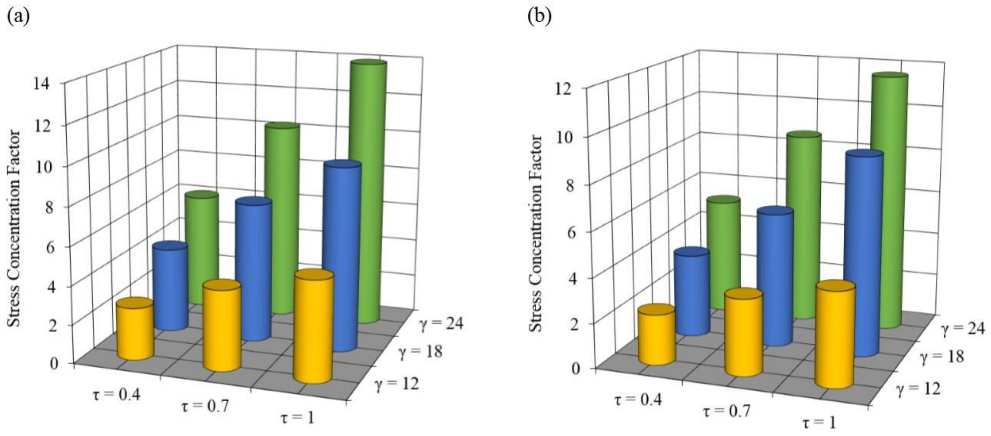

Fig. 7. The effect of the τ on the SCFs at different positions (β = 0.4, α = 16; 1st OPB moment loading condition): (a) Inner saddle, (b) Outer saddle

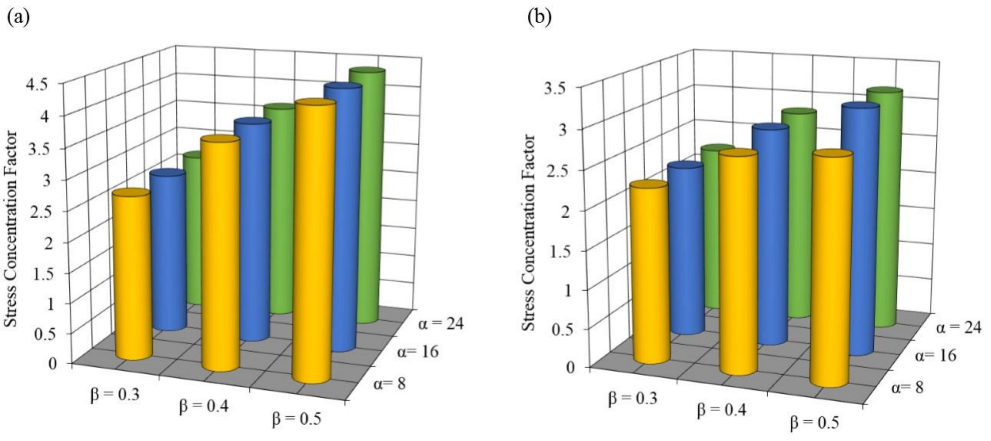

Fig. 8. The effect of the β on the SCFs at different positions (τ = 0.7, γ = 18; 1st OPB moment loading condition): (a) Inner saddle, (b) Outer saddle

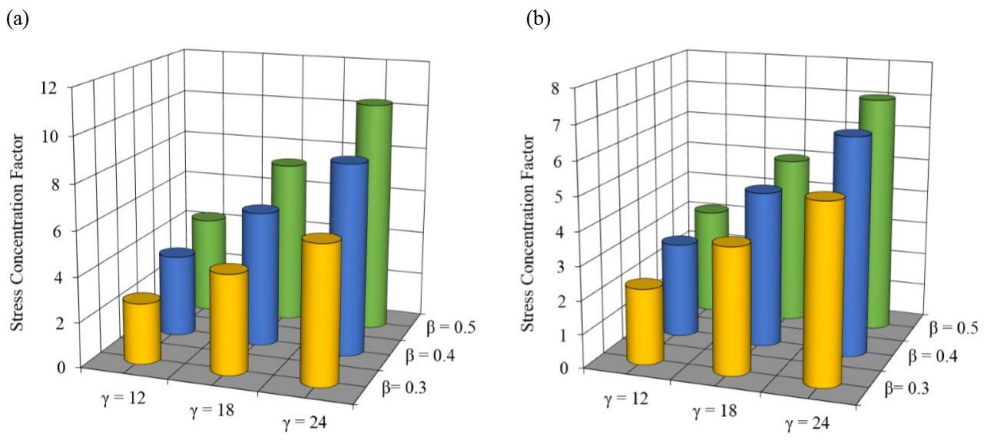

Fig. 9. The effect of the γ on the SCFs at different positions (α = 16, τ = 0.7; 1st OPB moment loading condition): (a) Inner saddle, (b) Outer saddle

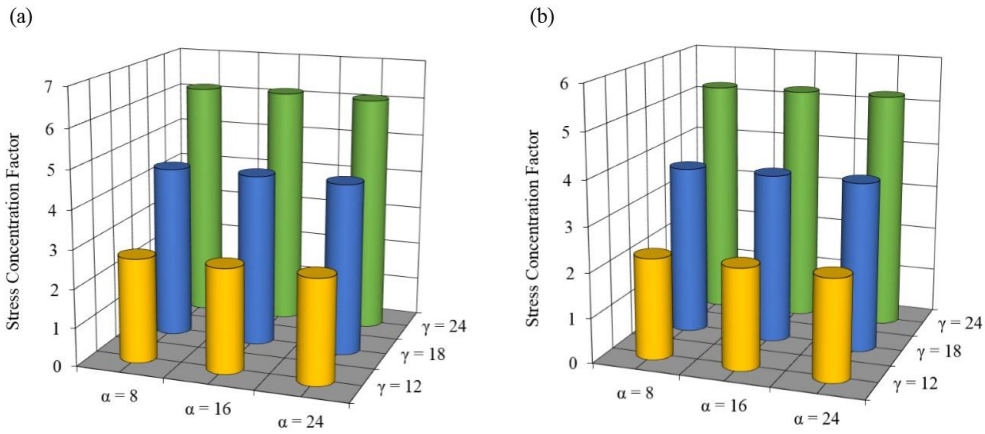

Fig. 10. The effect of the α on the SCFs at different positions (β = 0.4, τ = 0.7, 1st OPB moment loading condition): (a) Inner saddle, (b) Outer saddle

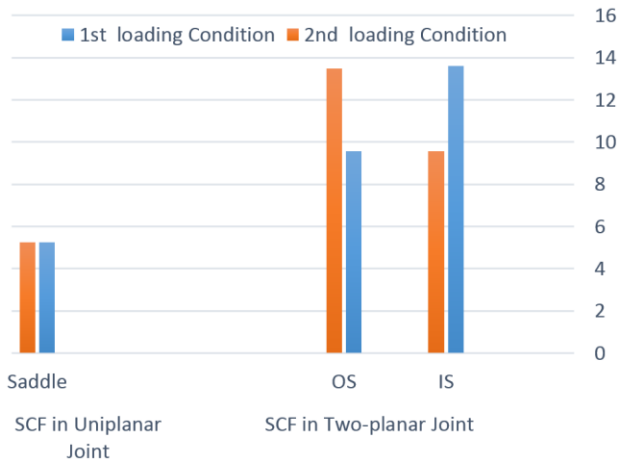

Fig. 11. Comparing the uniplanar and two-planar SCF values under the 1st and 2nd OPB moment loading conditions

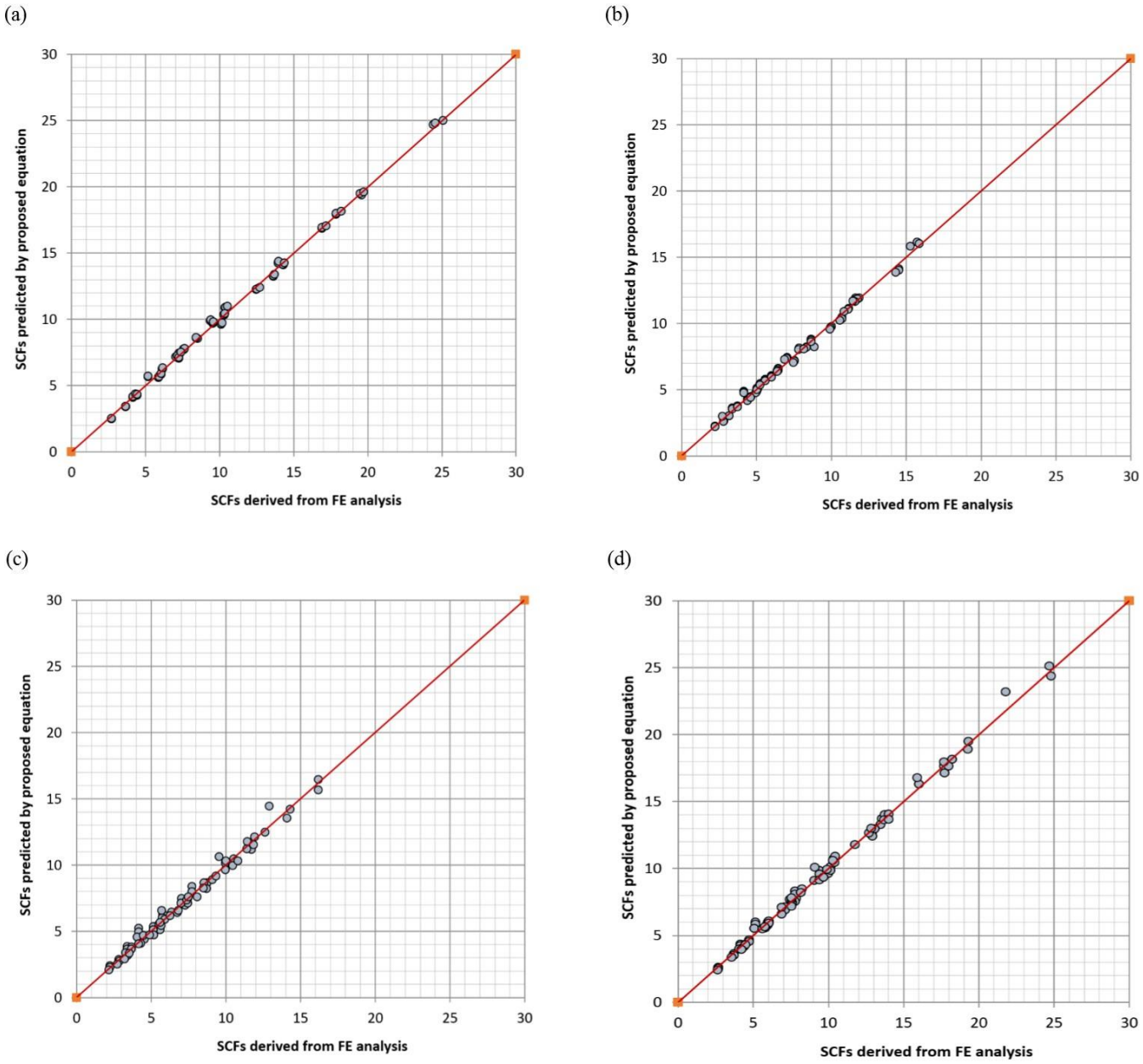

Fig. 12. Comparison of 81 SCF values calculated by the proposed equations with the corresponding SCFs extracted from the FE analysis: (a) Eq. (13), (b) Eq. (14), (c) Eq. (15), (d) Eq. (16)